4.2 Alumina A System

Anti-wear behavior exhibited by new additives within the three tribomonomer classes [1) A-R-B, 2) A-R-A + B-R'-B, and 3) Cyclic amides] in the steel system gave promise for further investigations in ceramics. Increased hardness and lower thermal conductivity of ceramic materials lead to higher surface temperatures which, combined with their chemical inertness, make evaluation in a ceramic system a demanding proving ground for anti-wear capability. The presentation of results from Alumina A testing begins with a presentation of hexadecane reference testing results and images in Section 4.2.1. Next, Section 4.2.2 compares results of several A-R-B tribomonomer wear tests with the hexadecane reference test average. Results from a pairing of A-R-A + B-R'-B additives are given in Section 4.2.3 followed in Section 4.2.4 by the results for the cyclic amide caprolactam.

4.2.1 Hexadecane Reference

Reference tests on six alumina ball and disk material pairs established a benchmark for comparison of additive effectiveness against hexadecane alone in the Alumina A system. The total wear volumes for the reference tests at this study's *standard* operating conditions of 0.25 m/s, 40 N, and 250 m sliding distance are presented in Figure 4.2.1.1. The noticeably large range of the reference test total wear volumes approaches an order of magnitude similar to the range of reference tests on steel. The heterogeneous properties associated with hot-pressing alumina into a rod may have induced these wear rate variances making a stable benchmark difficult to establish. The

average reference total wear volume of 27mm^3 is used for comparing individual additive tests. Regardless, the effect of the additives typically resulted in an order of magnitude total wear reduction even from the lowest reference test.

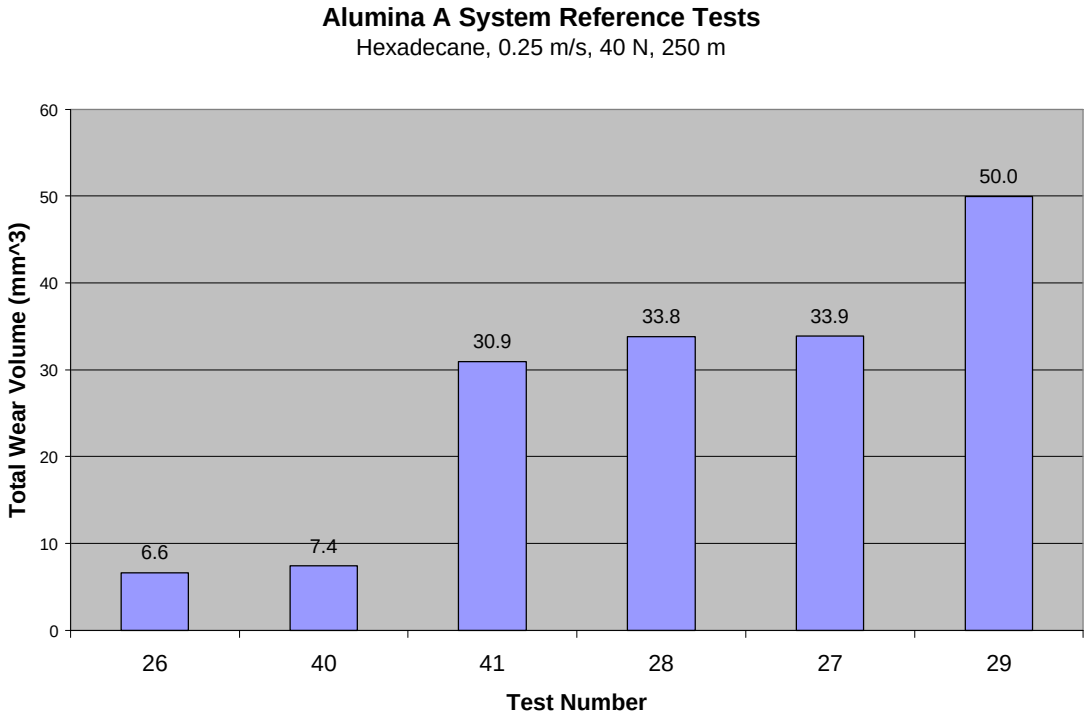

Figure 4.2.1.1 Alumina A System Hexadecane Reference Tests.

Photomacrographs for the reference tests are presented in Figures 4.2.1.2 – 7. Large amounts of wear debris are noticeable in the photomacrographs of the disk wear tracks. In comparing the wear tracks of Test 26 and Test 27 in Figures 4.2.1.2-3, the difference in the severity of wear is clearly visible. The first photomacrograph shows a uniform wear scar while the second reveals dark wear debris trapped sporadically throughout the wear scar. The same dark wear debris pattern appears in other high wear tests to varying degrees. Tests 28 and 29 resulted in large wear volumes and similar wear debris as shown in Figures 4.2.1.4-5. Figure 4.2.1.6 shows the smoother wear track of Test 40 coinciding with a lower wear volume. Shown in Figure 4.2.1.7 is the final

reference, Test 41, which resulted in a high wear volume with wear debris remaining in the wear track. The debris remained attached to the disk despite the fact that the disk was upside down and undergoing rotation during the test. Patchy discoloration evident inside several of the wear tracks remained even after ultrasonic rinsing in a solvent. High local temperatures and pressures may have caused this strong reattachment of the wear debris.

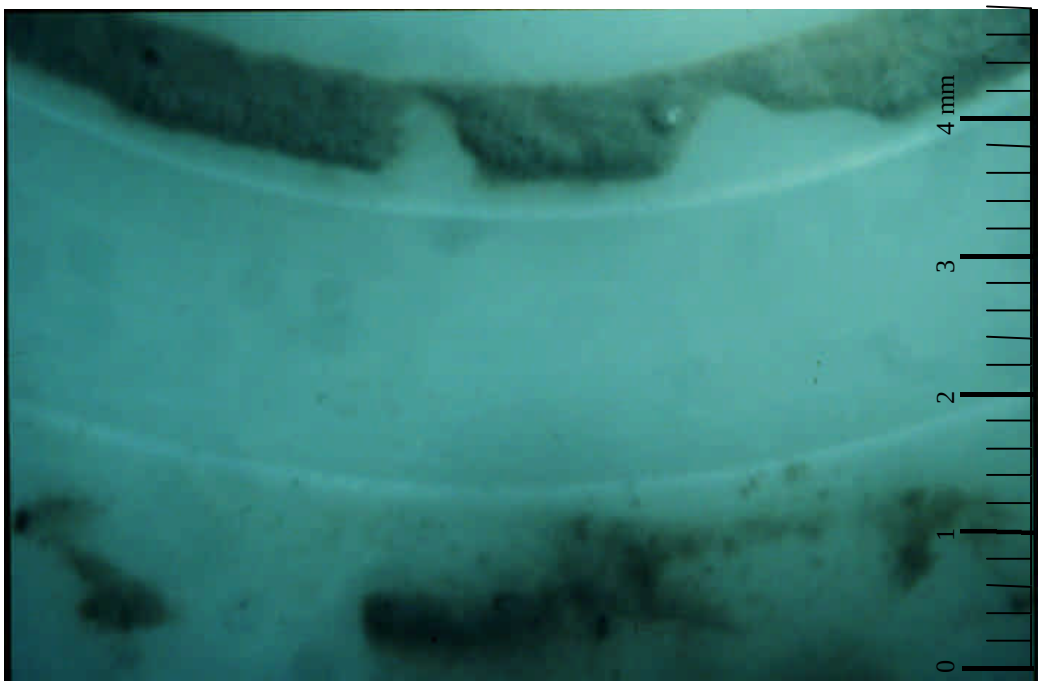

Figure 4.2.1.2 Alumina A System Reference, Test 26: Photomacrograph of Disk Wear Track (15.75 x)

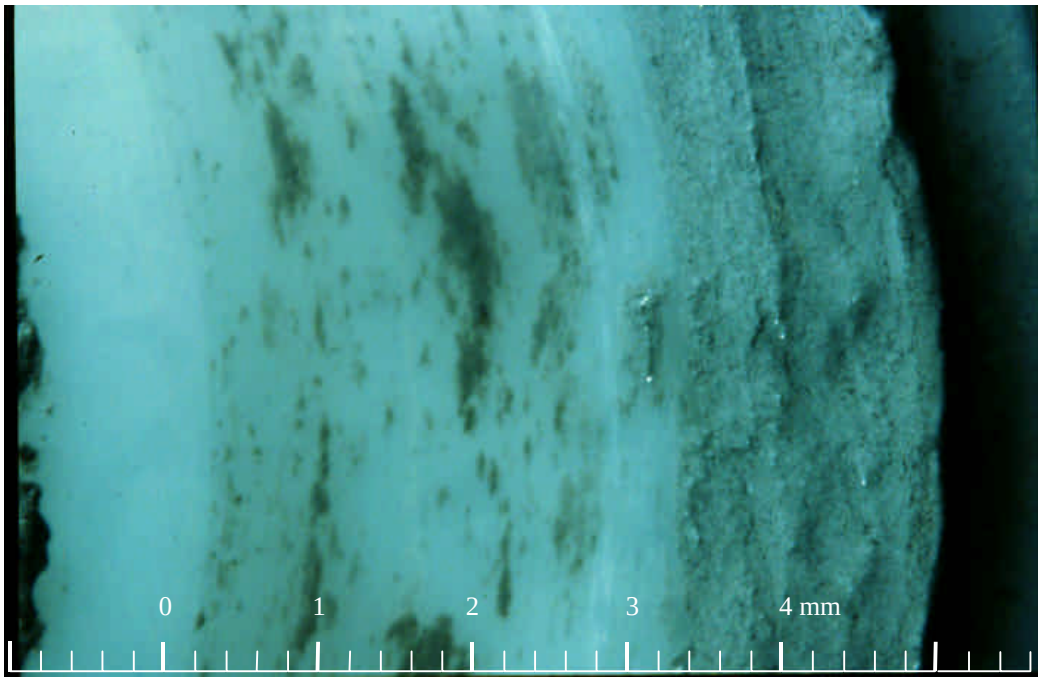

Figure 4.2.1.3 Alumina A System Reference, Test 27: Photomacrograph of Disk Wear Track (15.75 x)

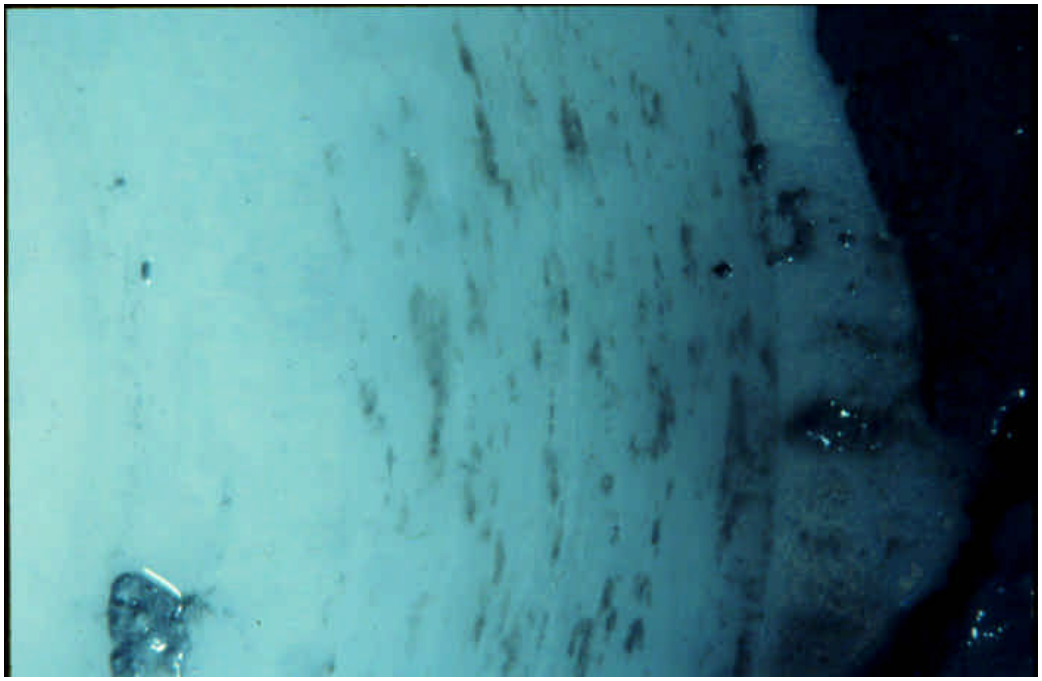

Figure 4.2.1.4 Alumina A System Reference, Test 28: Photomacrograph of Disk Wear Track (15.75 x)

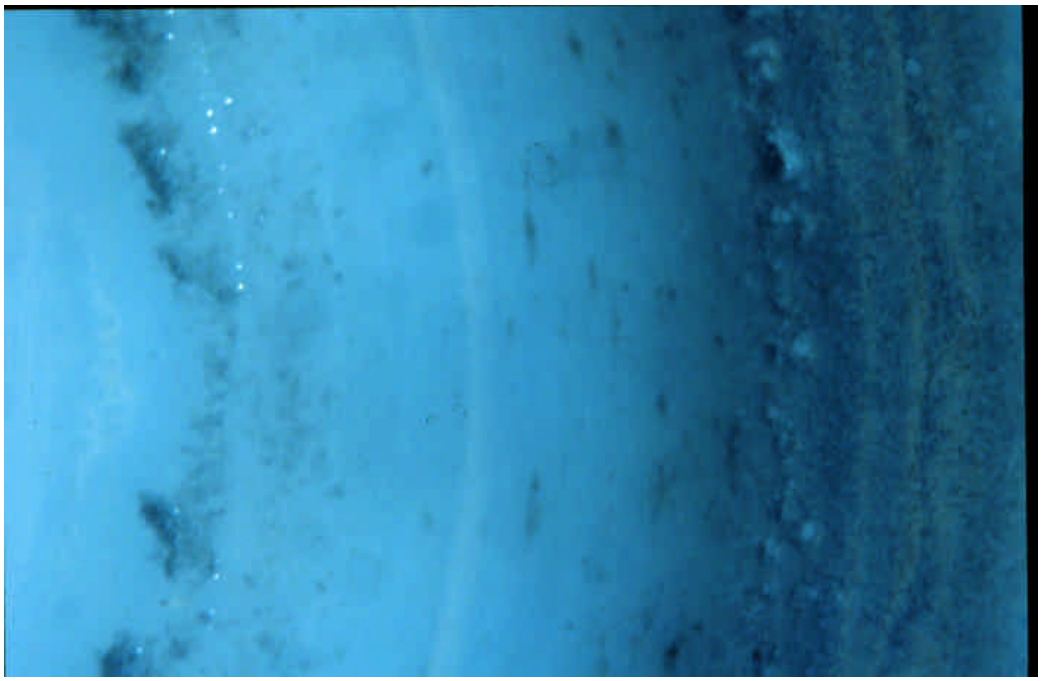

Figure 4.2.1.5 Alumina A System Reference, Test 29: Photomacrograph of Disk Wear Track (15.75 x)

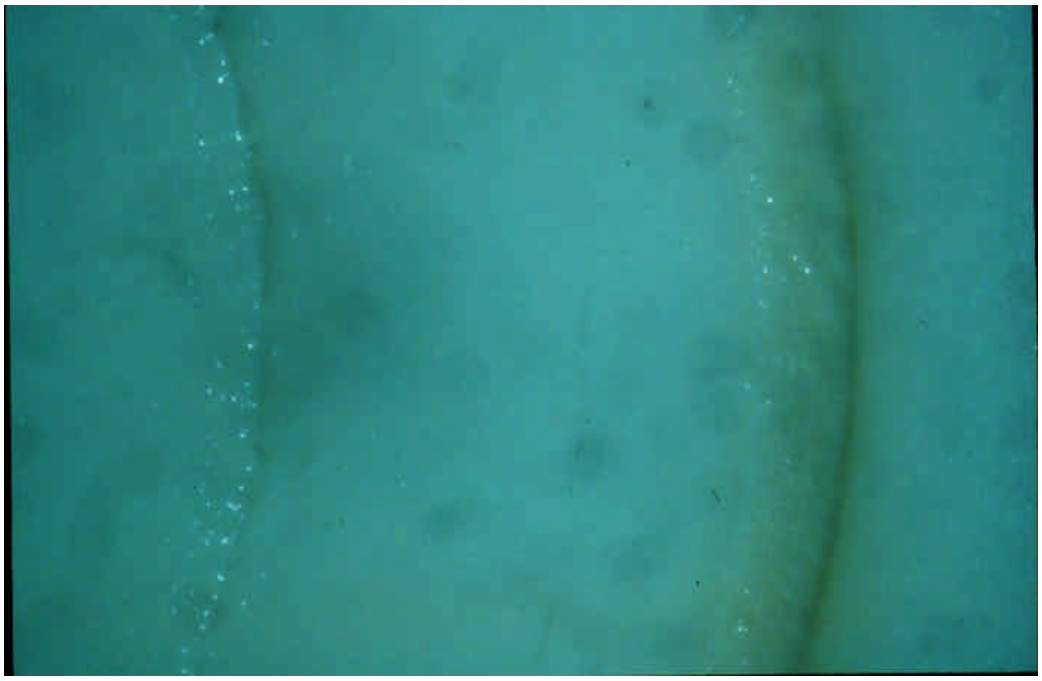

Figure 4.2.1.6 Alumina A System Reference, Test 40: Photomacrograph of Disk Wear Track (15.75 x)

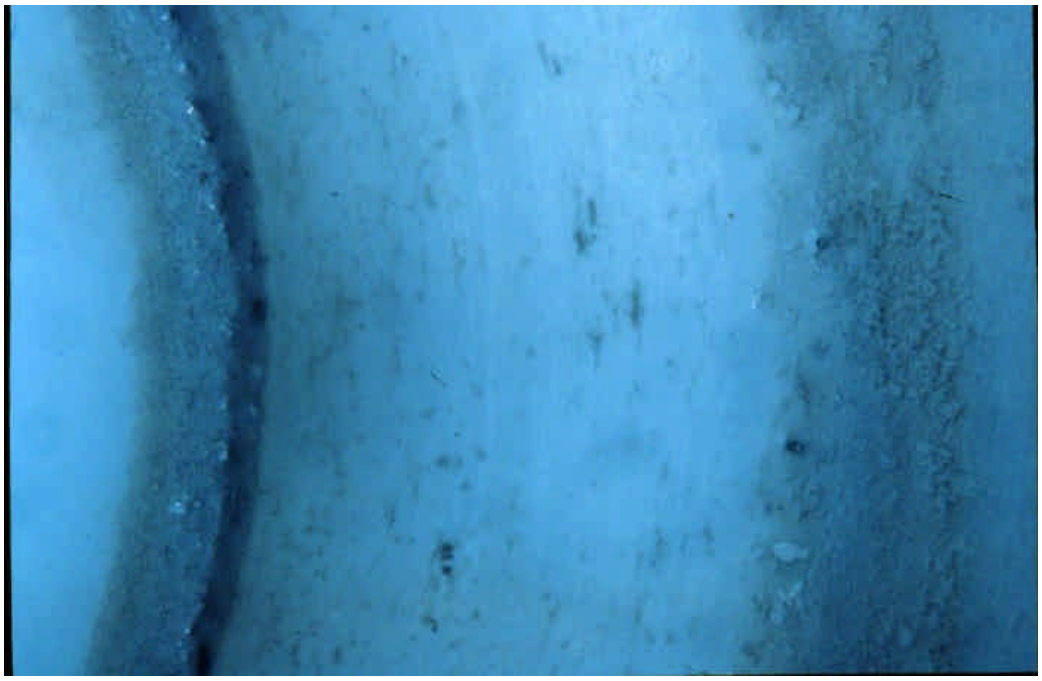

Figure 4.2.1.7 Alumina A System Reference, Test 41: Photomacrograph of Disk Wear Track (15.75 x)

4.2.2 A-R-B Type Tribomonomers

Testing in the Alumina A system spanned three classes of anti-wear additive candidates. The first of these classes was the A-R-B type of tribomonomers, which consisted of three aromatic compounds. Comparing the single wear test point of Figure 4.2.2.1 of the aromatic amino acid yields a marginal wear reduction of 33% compared to the material group reference. No photomacrographs are available from the wear specimens.

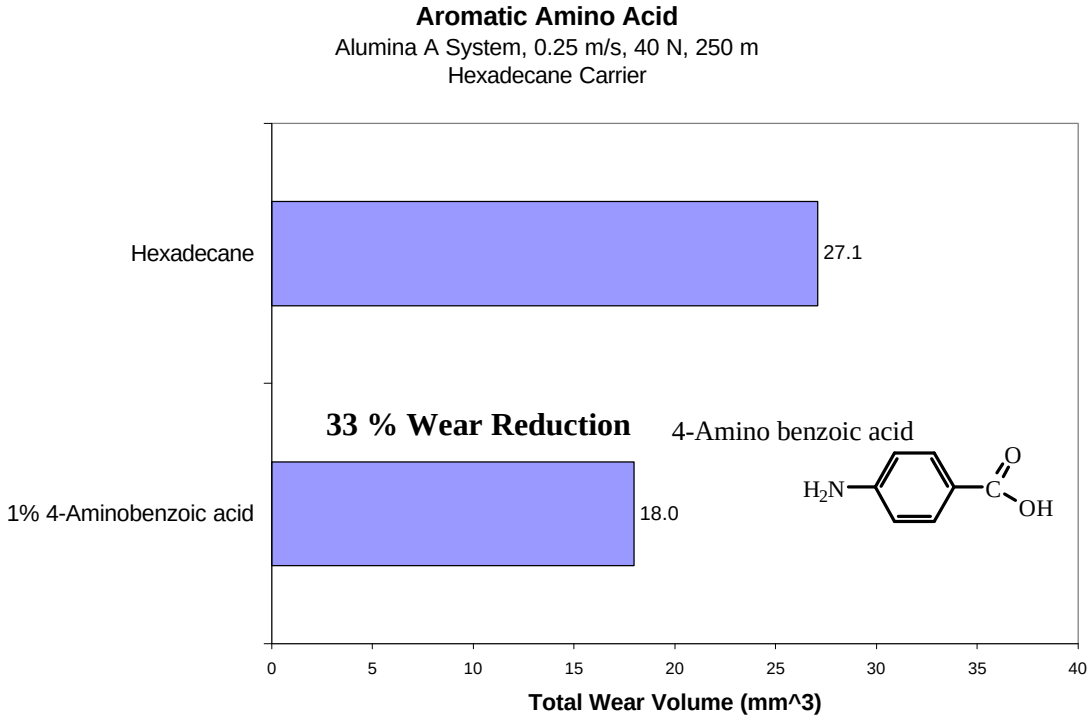

Figure 4.2.2.1 Anti-wear Effect of Aromatic Amino Acid in Alumina A System.

Changing the carboxylic acid group of the previous compound to an ester resulted in the wear reduction shown for ethyl-4-aminobenzoate in Figure 4.2.2.2. The single test of this compound gave significant wear reduction even after filtering. This suggests that effective anti-wear protection is provided by concentrations much less than the 1% of the original solution as the compound was only partially soluble. Photomacrographs of the 1% ethyl-4-aminobenzoate wear specimens are given in Figures 4.2.2.3-5. Yellow reaction products are present on the outer edges of the disk wear track in Figure 4.2.2.3. A patch of yellow is evident above the ball wear area as shown in Figure 4.2.2.4. The original compound and the hexadecane mixture were white indicating that a tribochemical reaction occurred in the presence of this compound to produce the yellow products. Direct internal lighting revealed the distribution and thickness of the reaction film on the disk wear track as shown in Figure 4.2.2.5.

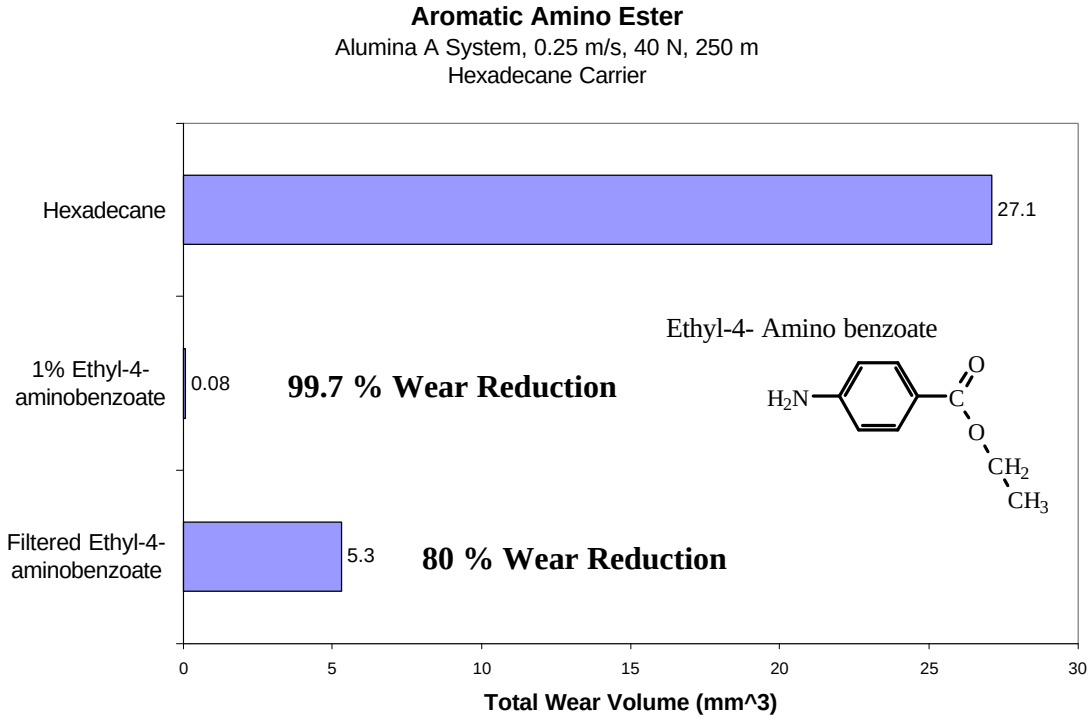

Figure 4.2.2.2 Anti-wear Effect of Aromatic Amino Ester in Alumina A System.

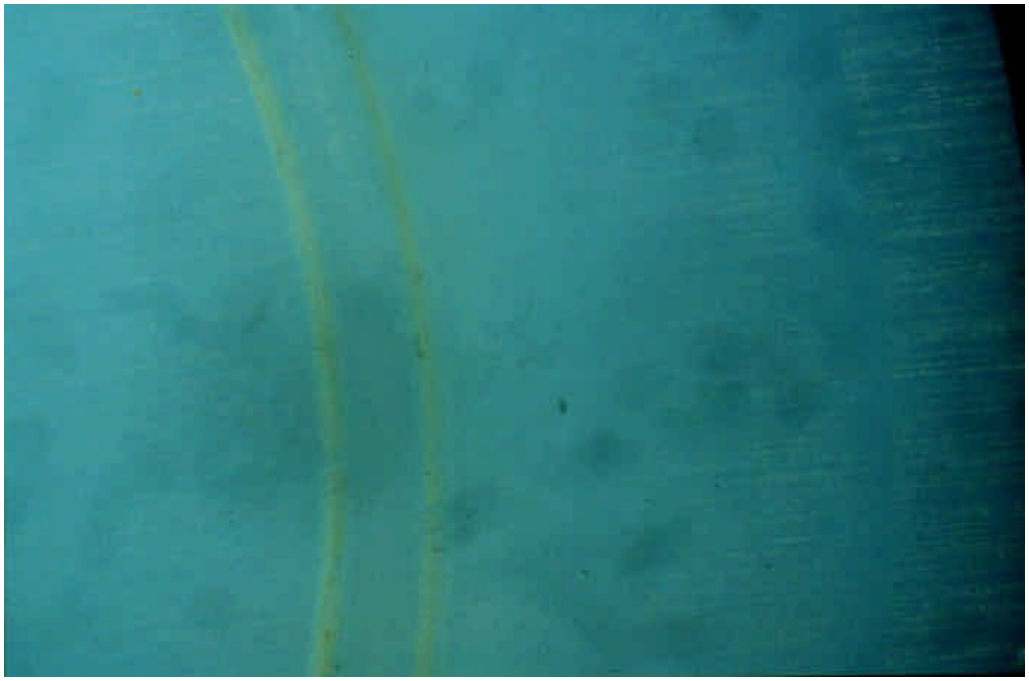

Figure 4.2.2.3 Ethyl-4-Amino Benzoate in Alumina A System, Test 32: Photomacrograph of Disk Wear Track (15.75 x)

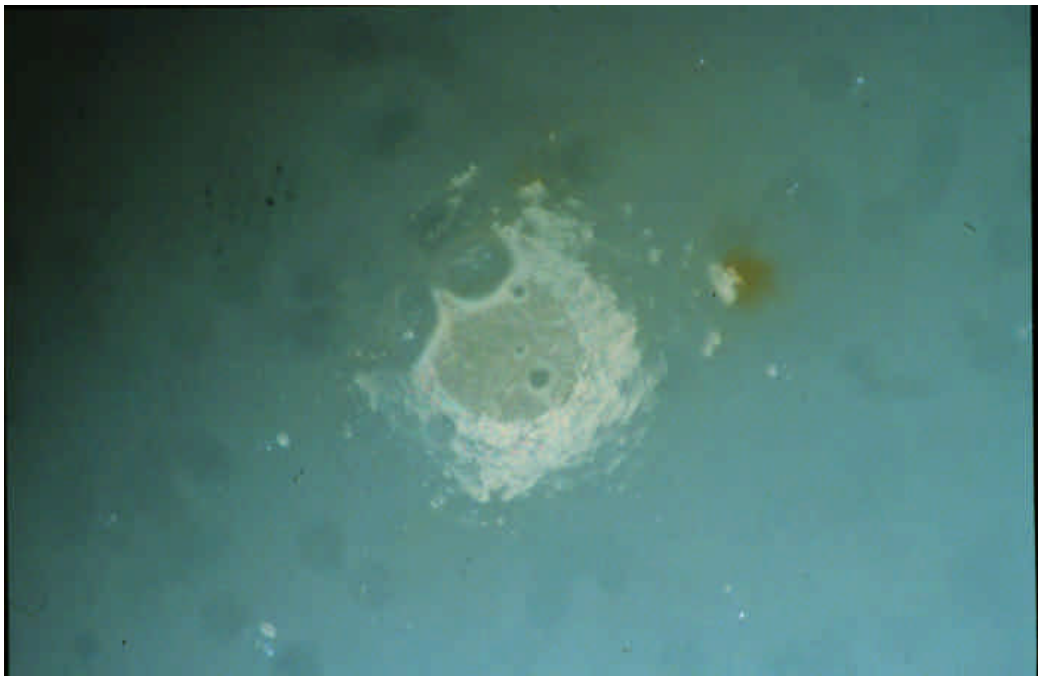

Figure 4.2.2.4 Ethyl-4-Amino Benzoate in Alumina A System, Test 32: Photomacrograph of Ball Wear Area (15.75 x)

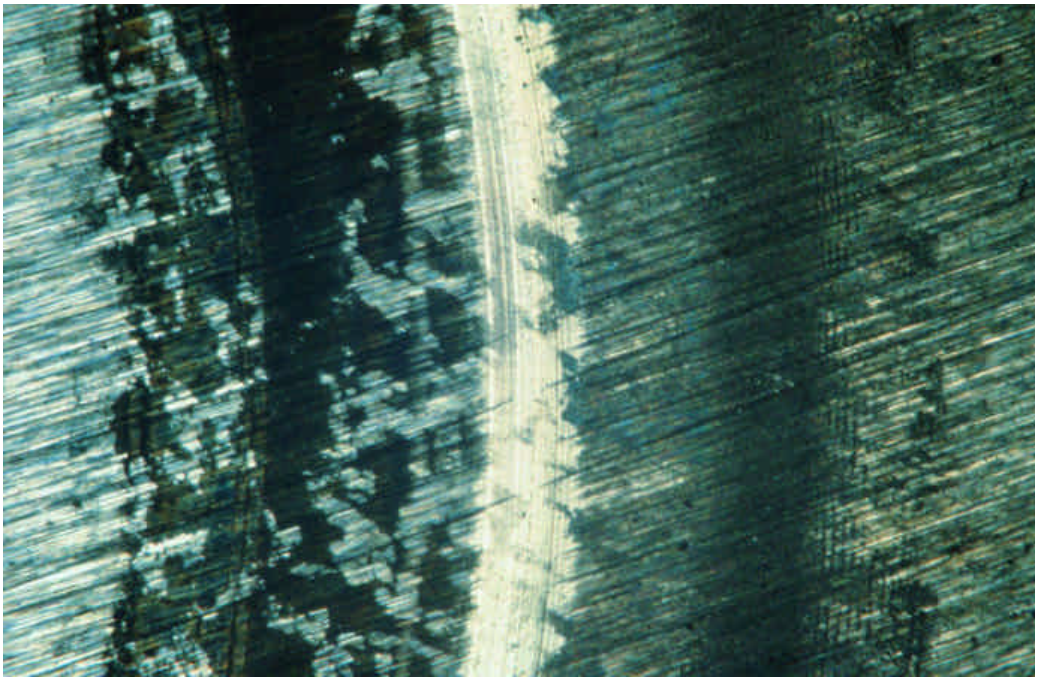

Figure 4.2.2.5 Ethyl-4-Amino Benzoate in Alumina A System, Test 33: Photomacrograph of Disk Wear Track (15.75 x)

Figures 4.2.2.6-9 show the wear areas for the filtered test. Filtration resulted in less visible film formation as depicted in Figure 4.2.2.6. Interesting photomacrographs of the ball wear scar in Figures 4.2.2.7-9 document remarkable evidence of an attached debris layer. Figure 4.2.2.7 reveals a slight yellowish reaction product around the edge of the ball wear scar and large amounts of fine debris deposited away from the contact area. A combination of direct internal and indirect external lighting reveals the nature of the layer as the lower half of the ball wear scar reflects light and reveals its smooth nature in Figure 4.2.2.8. The upper portion of the ball wear scar scatters the direct light and indicates a rougher surface after apparent flaking, spalling, delamination or other removal of a portion of the compacted debris layer. Figure 4.2.2.9 shows the formation of a crack in the debris layer under higher magnification, which suggests a delamination wear mechanism is responsible for removal of the compacted debris layer.

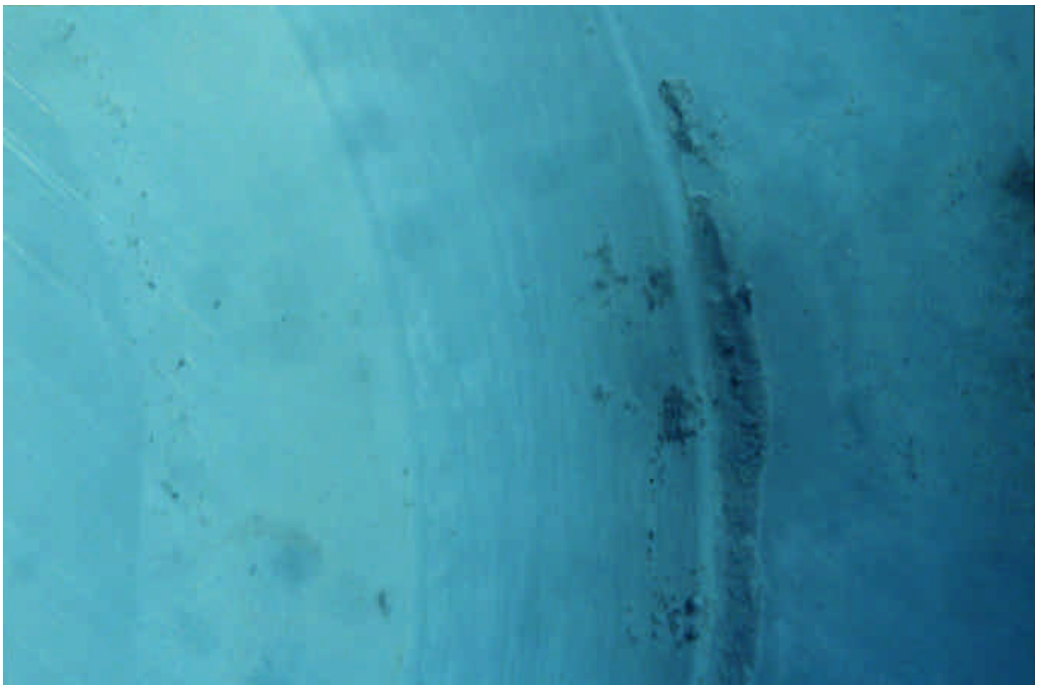

Figure 4.2.2.6 Filtered Ethyl-4-Amino Benzoate in Alumina A System, Test 42: Photomacrograph of Disk Wear Track (15.75 x)

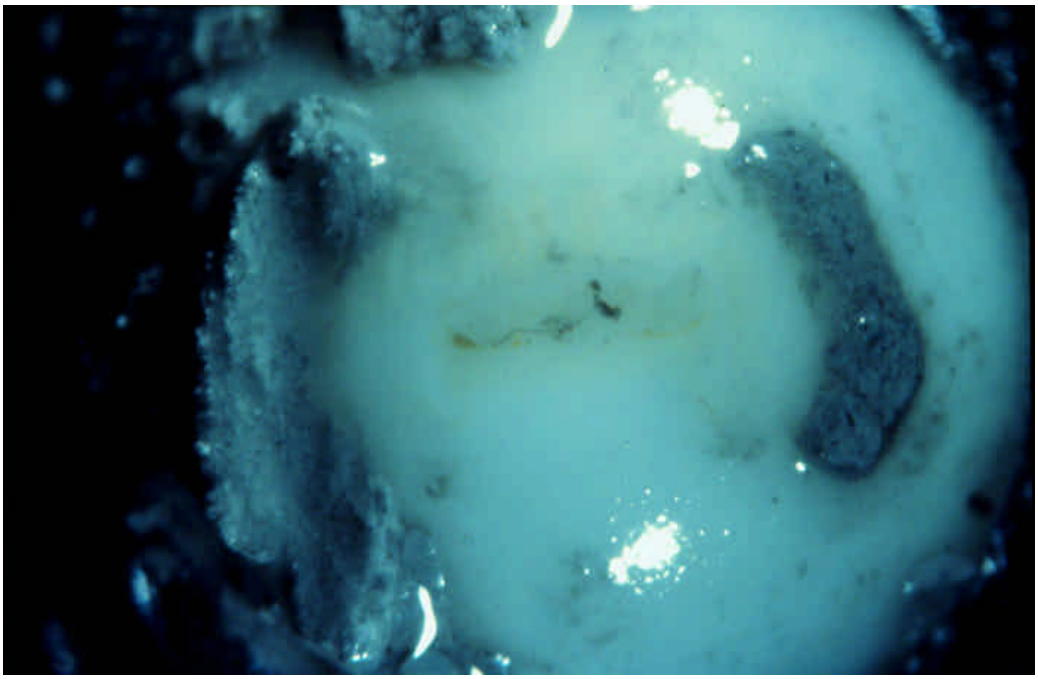

Figure 4.2.2.7 Filtered Ethyl-4-Amino Benzoate in Alumina A System, Test 42: Photomacrograph of Ball Wear Area (15.75 x)

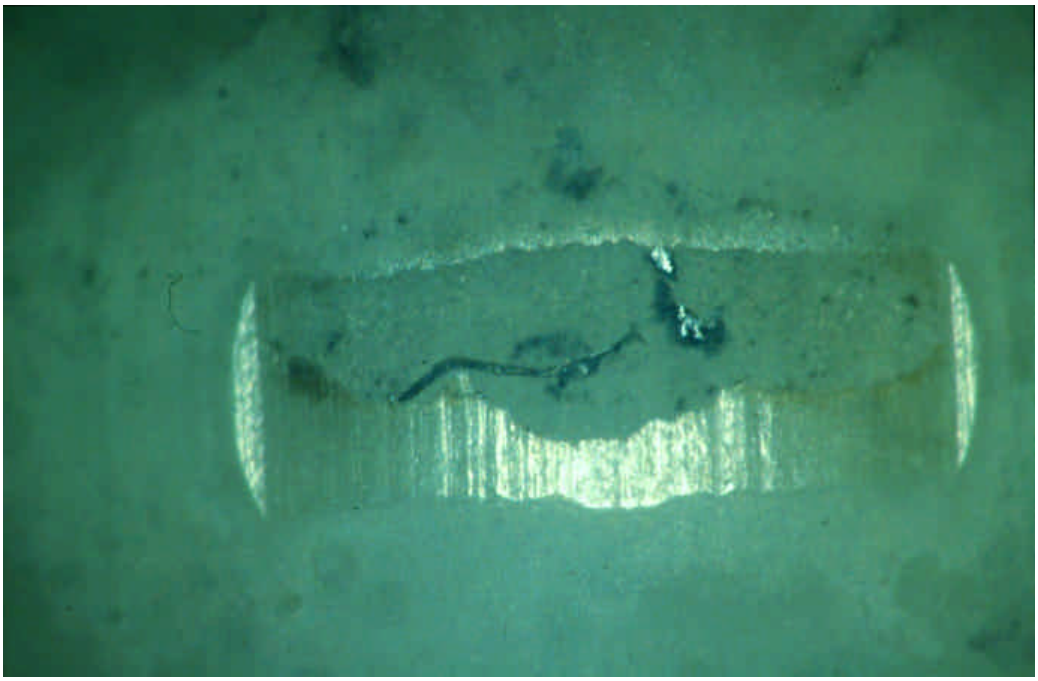

Figure 4.2.2.8 Filtered Ethyl-4-Amino Benzoate in Alumina A System, Test 42: Photomacrograph of Ball Wear Area (40 x)

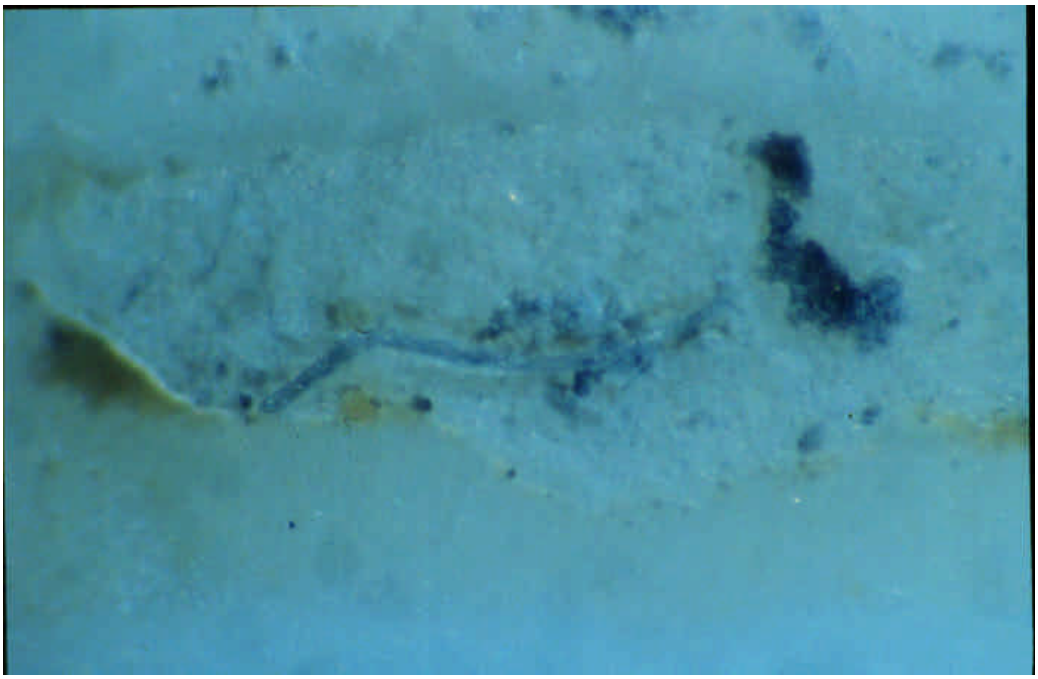

Figure 4.2.2.9 Filtered Ethyl-4-Amino Benzoate in Alumina A System, Test 42: Photomacrograph of Ball Wear Area (80 x)

Changing the amino group from ethyl-4-aminobenzoate and replacing it with a hydroxyl group results in a compound similar to that shown in Figure 4.2.2.10. The single point wear reduction estimate for this compound was significant yet slightly lower than its amino counterpart. However, extremely interesting wear areas resulted.

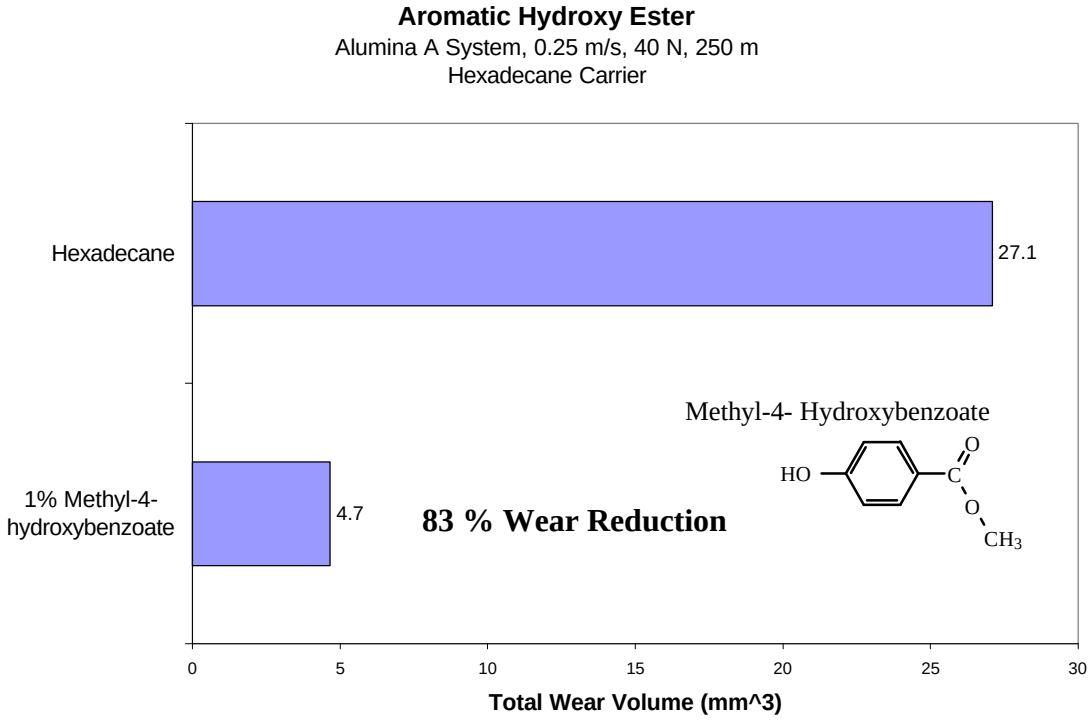

Figure 4.2.2.10 Anti-wear Effect of Aromatic Hydroxy Ester in Alumina A System.

The photomacrograph of Figure 4.2.2.11 shows typical wear debris alongside the disk wear track. Remarkable evidence of a ball debris reaction layer appears in Figures 4.2.2.12-14, where at various magnifications a fingerlike detachment is seen breaking off of the top of the ball wear scar.

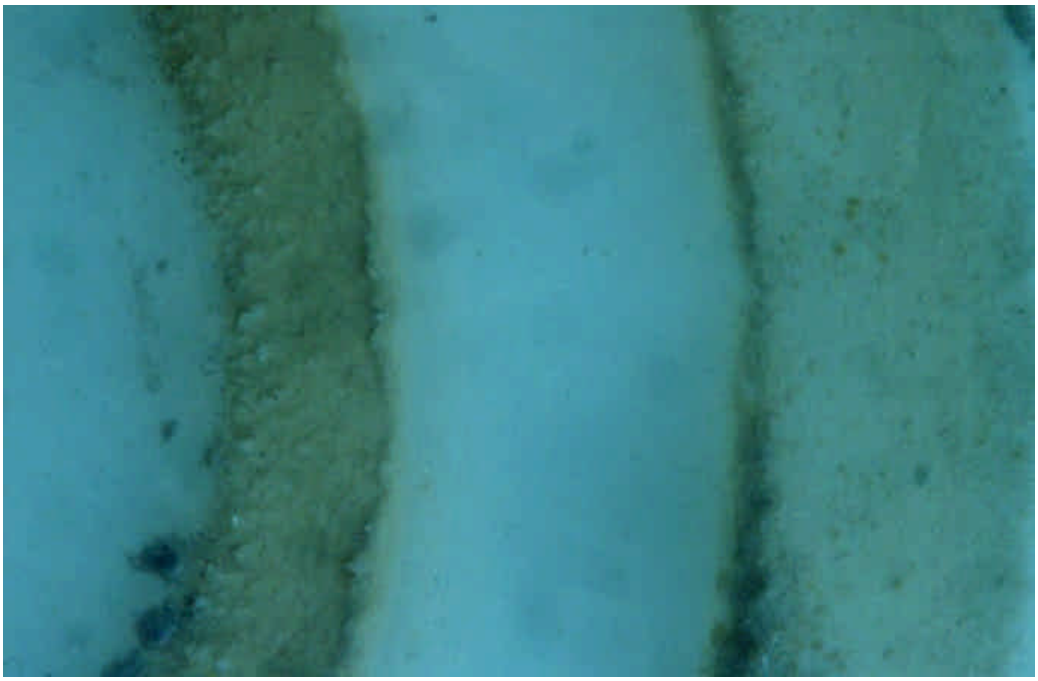

Figure 4.2.2.11 Methyl-4-Hydroxy Benzoate in Alumina A System, Test 34: Photomacrograph of Disk Wear Track (15.75 x)

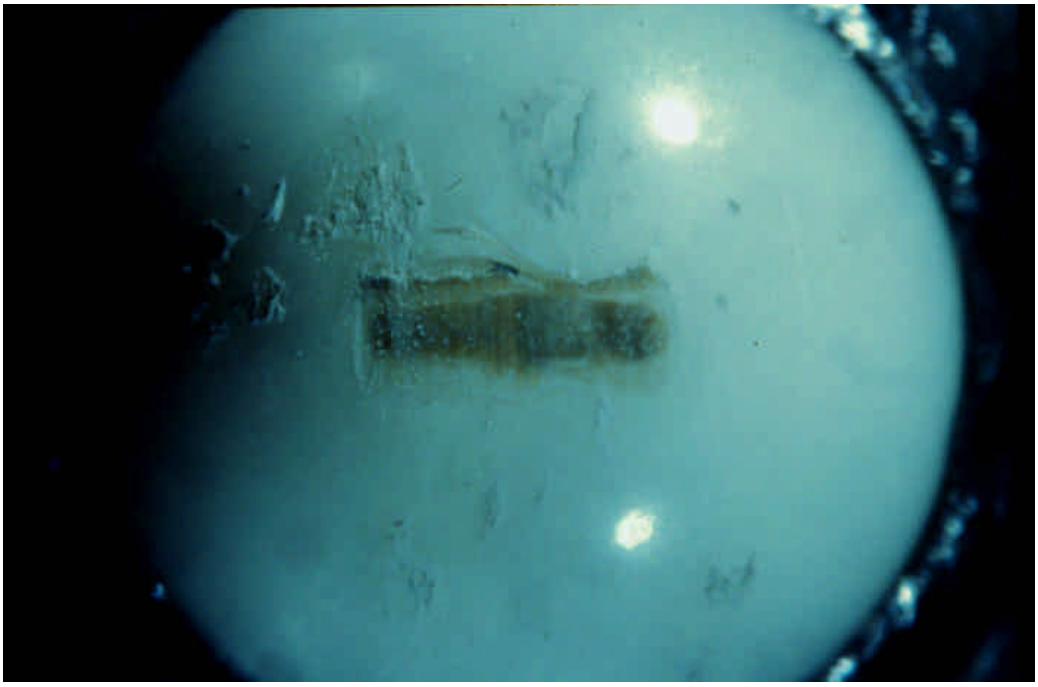

Figure 4.2.2.12 Methyl-4-Hydroxy Benzoate in Alumina A System, Test 34: Photomacrograph of Ball Wear Area (15.75 x)

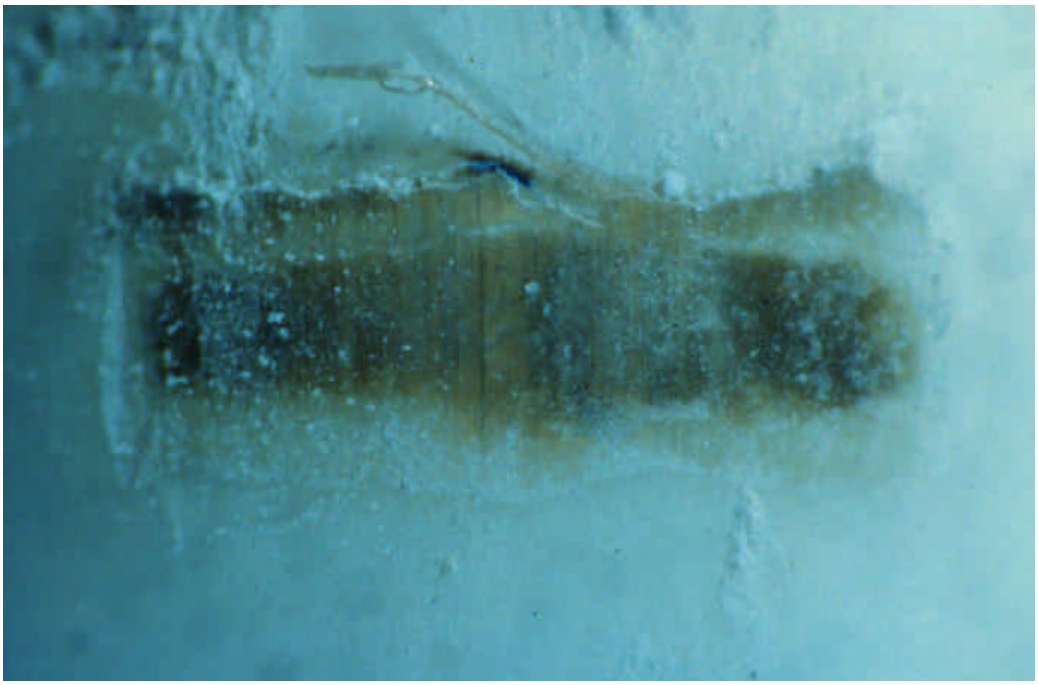

Figure 4.2.2.13 Methyl-4-Hydroxy Benzoate in Alumina A System, Test 34: Photomacrograph of Ball Wear Area (40 x)

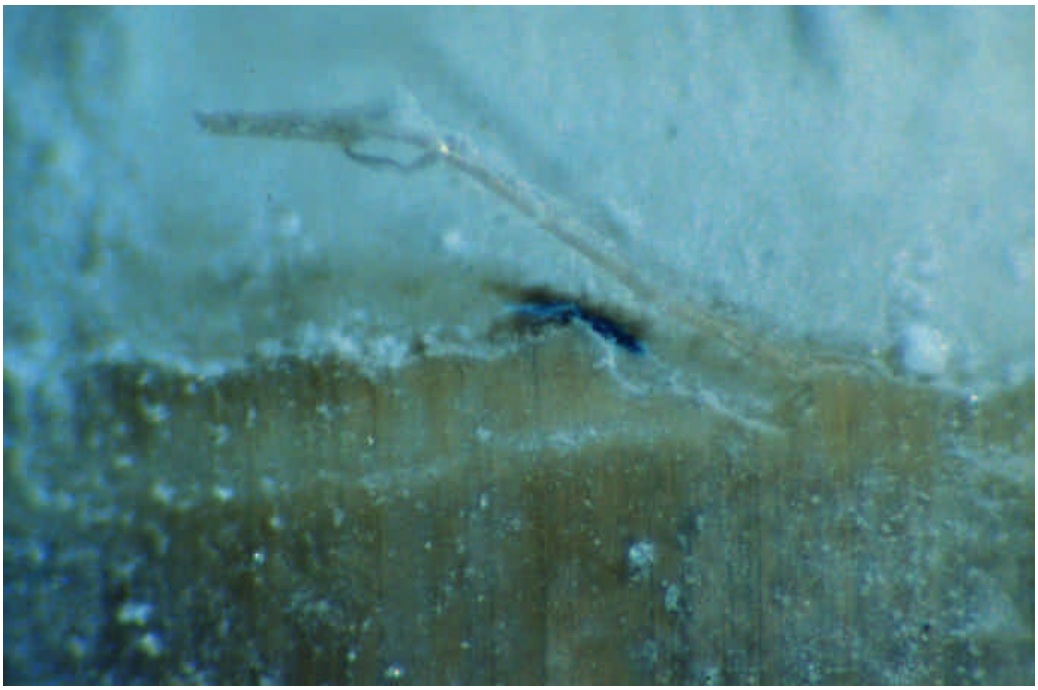

Figure 4.2.2.14 Methyl-4-Hydroxy Benzoate in Alumina A System, Test 34: Photomacrograph of Ball Wear Area (80 x)

4.2.3 A-R-A + B-R'-B Type Compounds

The average result of two tests of the equimolar mixture of the A-R-A + B-R'-B compounds is depicted in Figure 4.2.3.1. Excellent anti-wear behavior of this mixture was observed at 1% and after a single test of the filtered mixture.

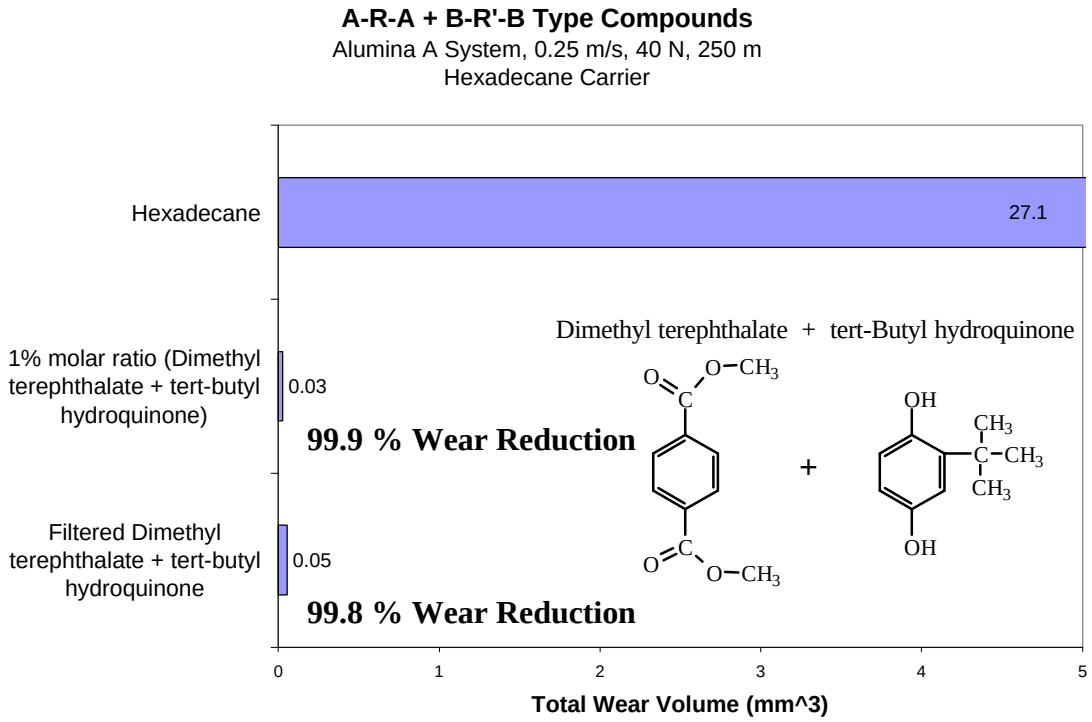

Figure 4.2.3.1 Anti-wear Effect of A-R-A + B-R'-B Compounds Dimethyl Terephthalate and Tert-Butyl Hydroquinone in Alumina A System.

Photomacrographs of the disk wear tracks in Figures 4.2.3.2-4 show dark tribochemical reaction products at the edges of the contact zone. The inner track (left-most) of Figure 4.2.3.2 is likely a hydrodynamic artifact representing the edge of the wake from the ball. However, it reveals that the debris is attracted sufficiently to the disk to lightly reattach given conditions other than high-pressure tribological contact. Figure 4.2.3.3 shows orderly edges of lightly reattached debris formed away from the contact zone. The presence of similar artifacts in other photomacrographs suggests a charged

nature of the debris as it clings to the disk surface. Figure 4.2.3.4 shows the reflective nature of a portion of the disk wear track under higher magnification and direct internal lighting. Rinsing the ball wear area with hexane left some debris directly on the scar as shown in Figures 4.2.3.5 - 6. Figure 4.2.3.7 shows the same area after wiping with lab tissue. The ball wear photomacrograph from a similar test in Figure 4.2.3.8 shows slightly darker debris at the upper edge of the scar.

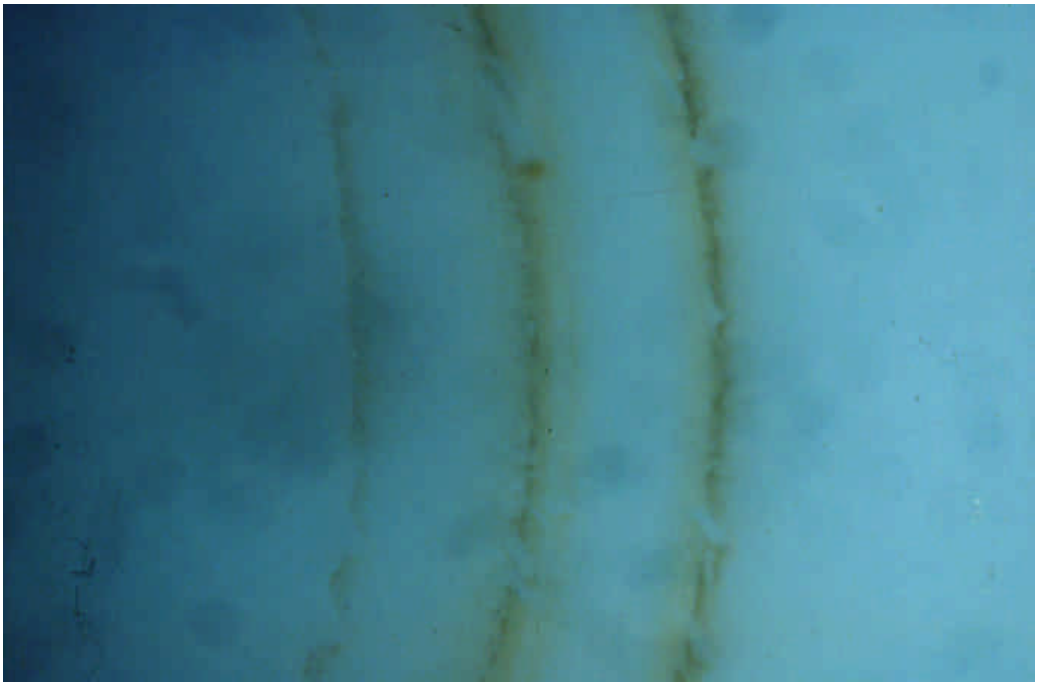

Figure 4.2.3.2 Dimethyl Terephthalate and Tert-Butyl Hydroquinone in Alumina A System, Test 38: Photomacrograph of Disk Wear Track (15.75 x)

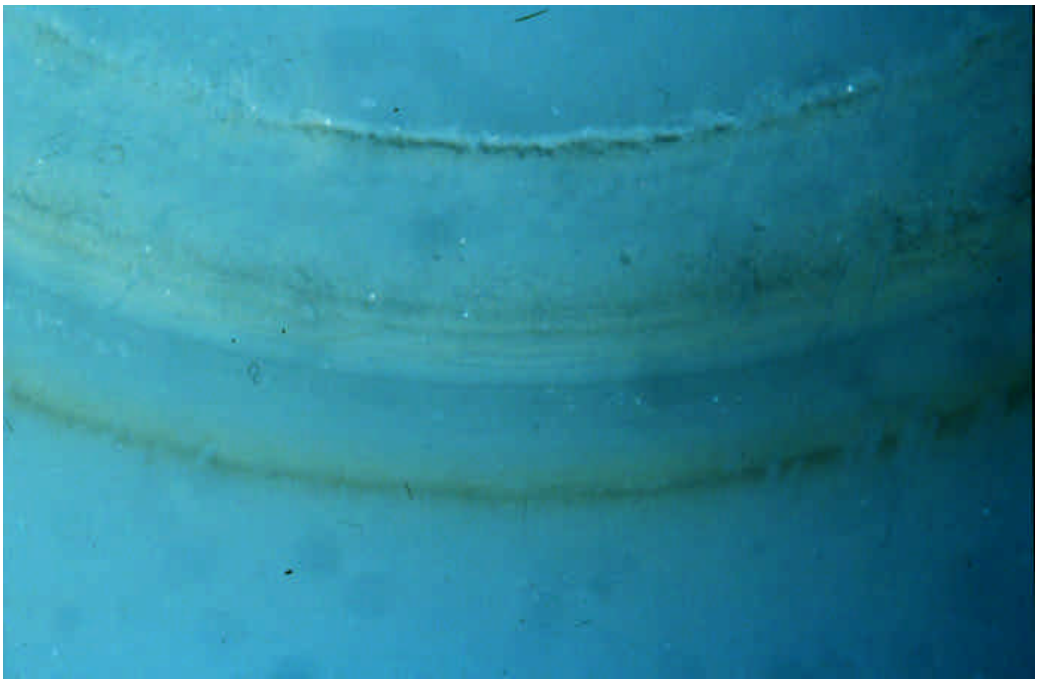

Figure 4.2.3.3 Dimethyl Terephthalate and Tert-Butyl Hydroquinone in Alumina A System, Test 38: Photomacrograph of Disk Wear Track (15.75 x)

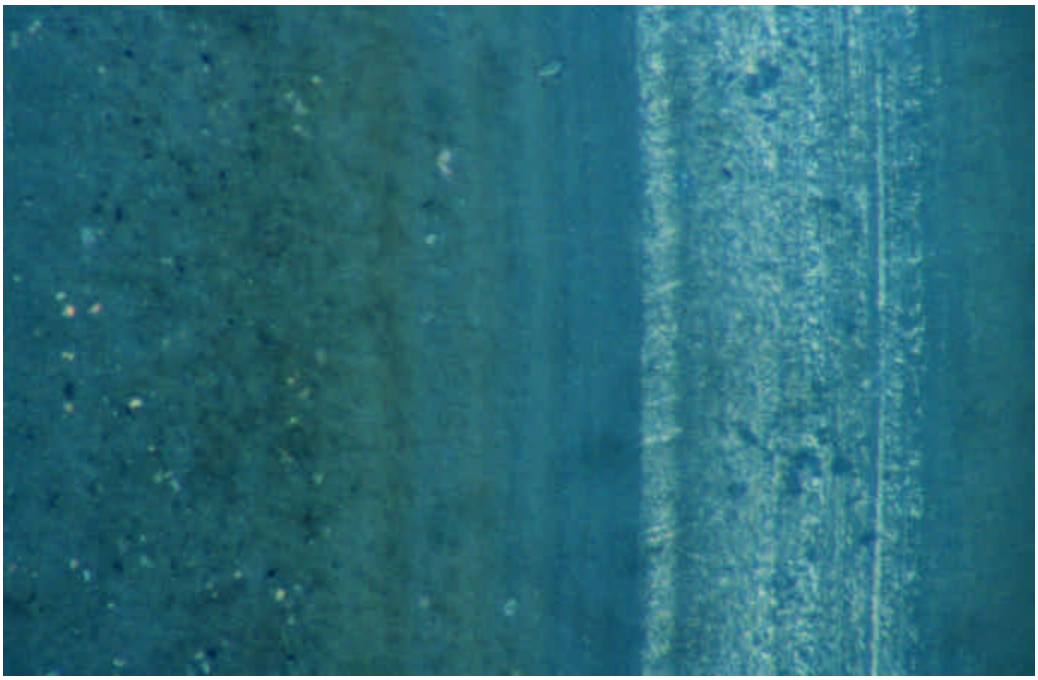

Figure 4.2.3.4 Dimethyl Terephthalate and Tert-Butyl Hydroquinone in Alumina A System, Test 38: Photomacrograph of Disk Wear Track (40 x)

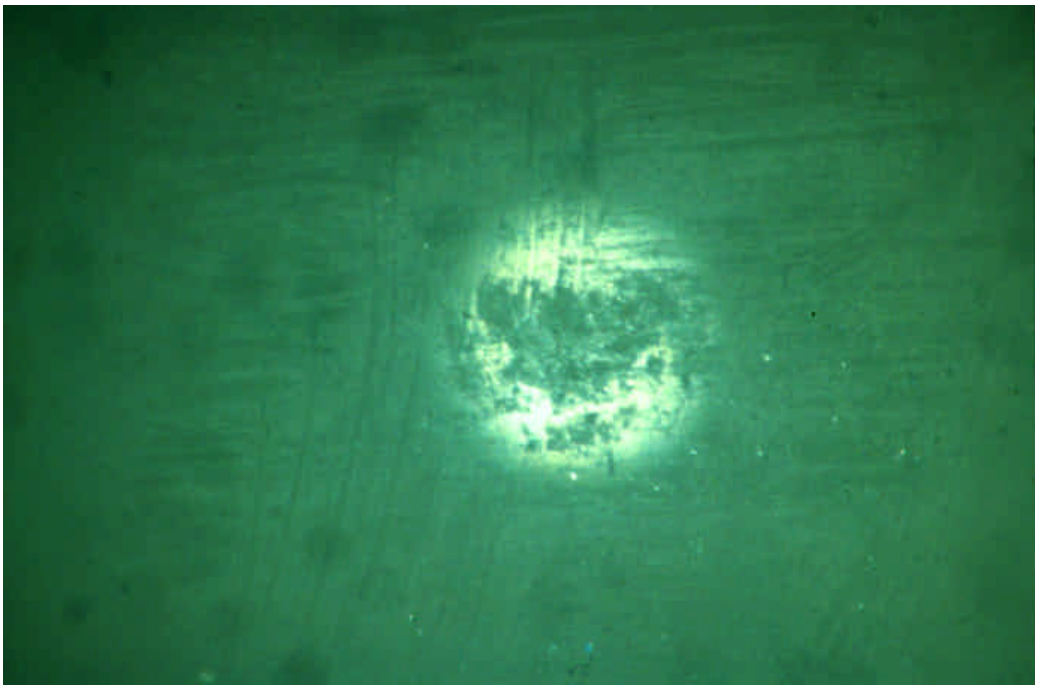

Figure 4.2.3.5 Dimethyl Terephthalate and Tert-Butyl Hydroquinone in Alumina A System, Test 38: Photomacrograph of Ball Wear Area (40 x)

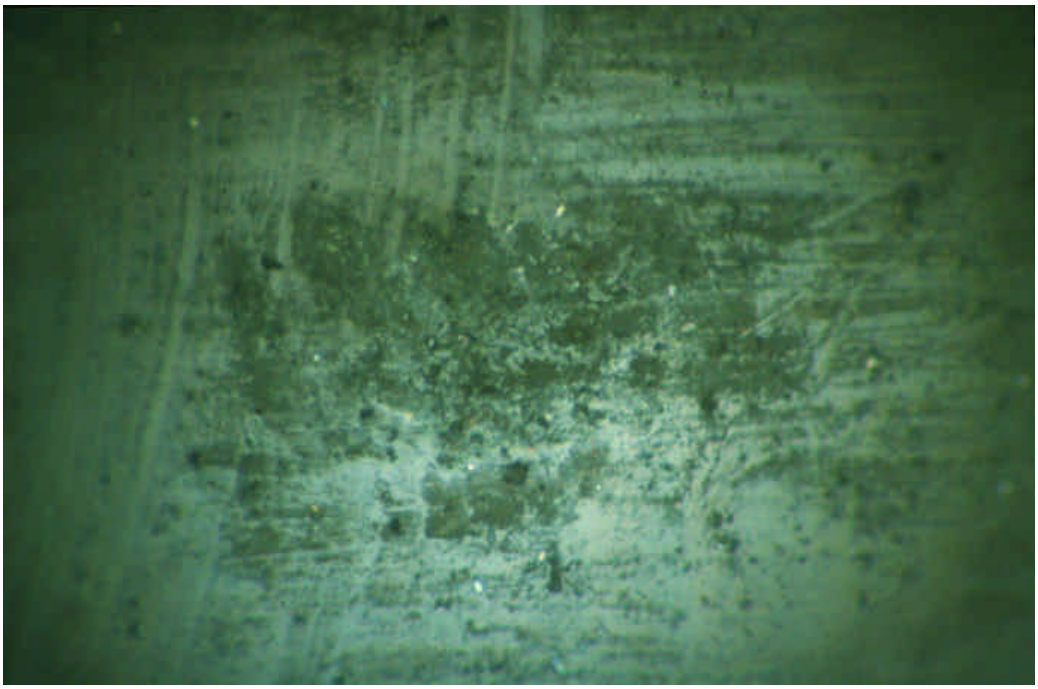

Figure 4.2.3.6 Dimethyl Terephthalate and Tert-Butyl Hydroquinone in Alumina A System, Test 38: Photomacrograph of Ball Wear Area (80 x)

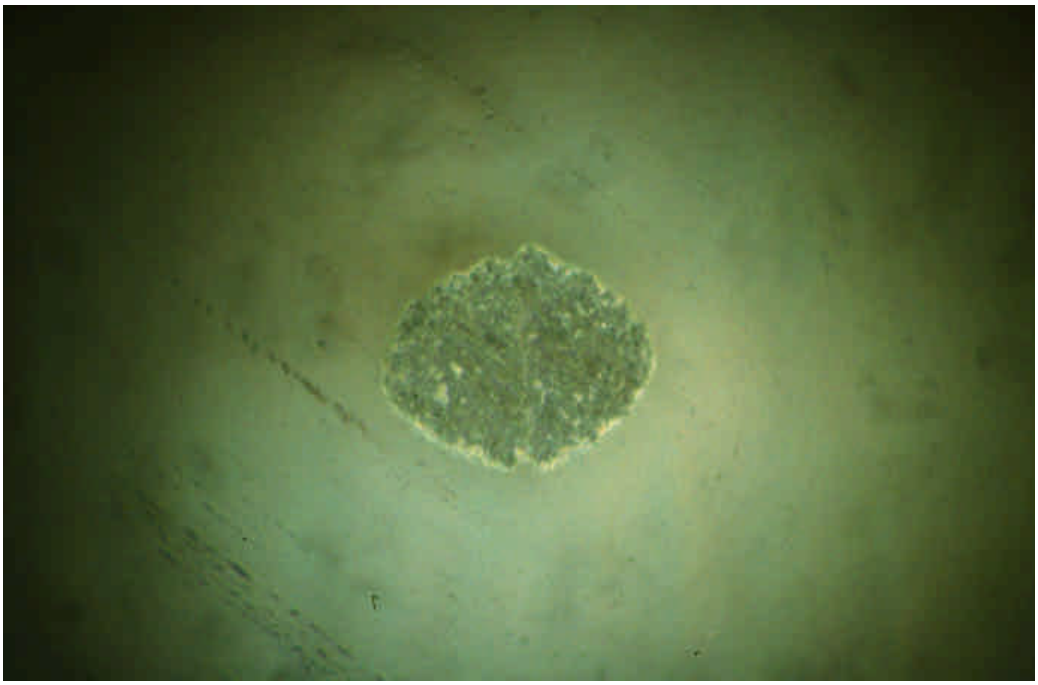

Figure 4.2.3.7 Dimethyl Terephthalate and Tert-Butyl Hydroquinone in Alumina A System, Test 38: Photomacrograph of Ball Wear Area (80 x)

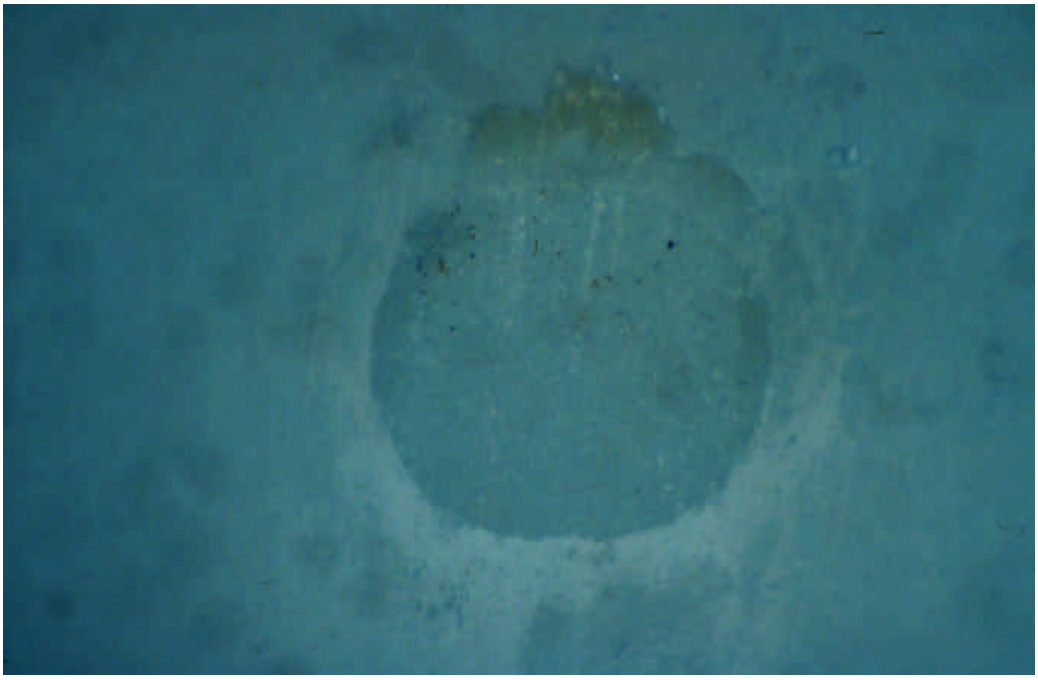

Figure 4.2.3.8 Dimethyl Terephthalate and Tert-Butyl Hydroquinone in Alumina A System, Test 39: Photomacrograph of Ball Wear Area (80 x)

Filtration of the mixture of dimethyl terephthalate and tert-butyl hydroquinone resulted in similar wear reductions. Figures 4.2.3.9-10 show an even and fine distribution of debris and/or compound covering the surface. Centrifugal effects probably prevented the material from reaching the inner (left) portion of the disk surface as shown in Figure 4.2.3.9. The edge of the outer ring (right) represents the area where the specimen was in contact with the disk holder. In Figure 4.2.3.10, two bands appear near the wear track which are distinctly darker than the outer ring. This suggests that dissipating thermal energy near the contact zone enhances adsorption of the additive and/or wear debris. The ball wear area of Figure 4.2.3.11 partially reflects the direct internal lighting and thus reveals a thin covering of adsorbed species on and near the ball wear scar as well.

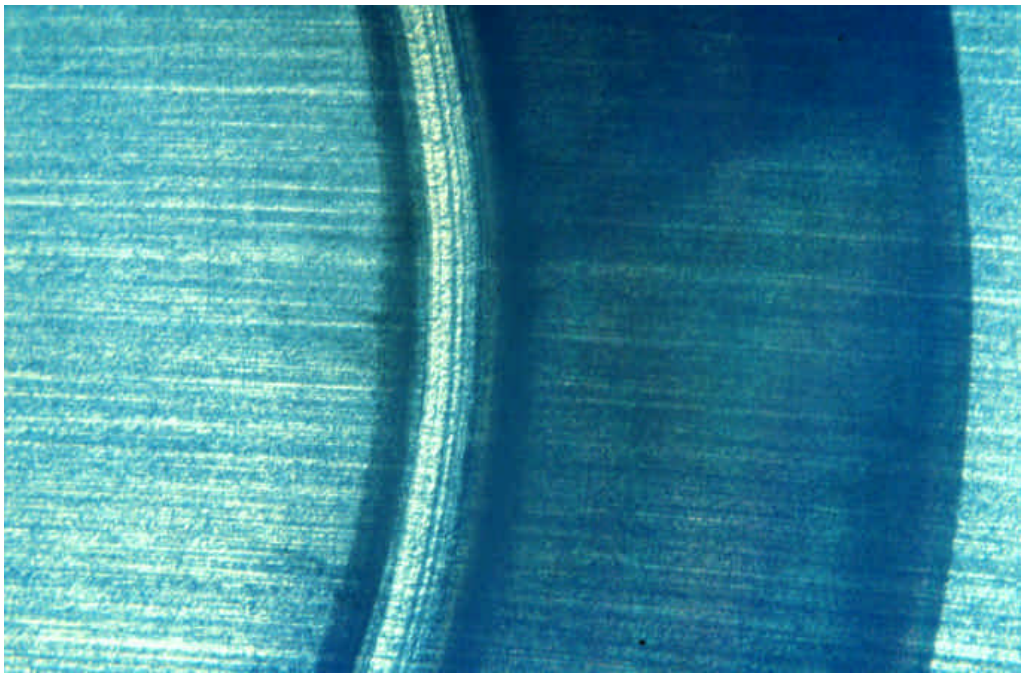

Figure 4.2.3.9 Filtered Dimethyl Terephthalate and Tert-Butyl Hydroquinone in Alumina A System, Test 44: Photomacrograph of Disk Wear Track (15.75 x)

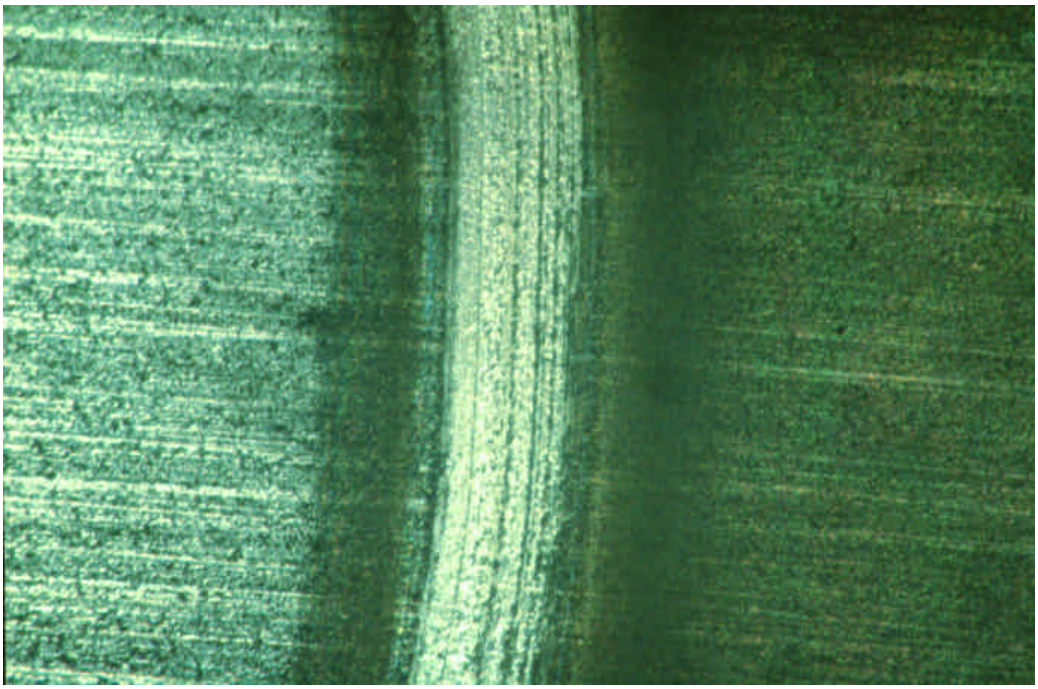

Figure 4.2.3.10 Filtered Dimethyl Terephthalate and Tert-Butyl Hydroquinone in Alumina A System, Test 44: Photomacrograph of Disk Wear Track (40 x)

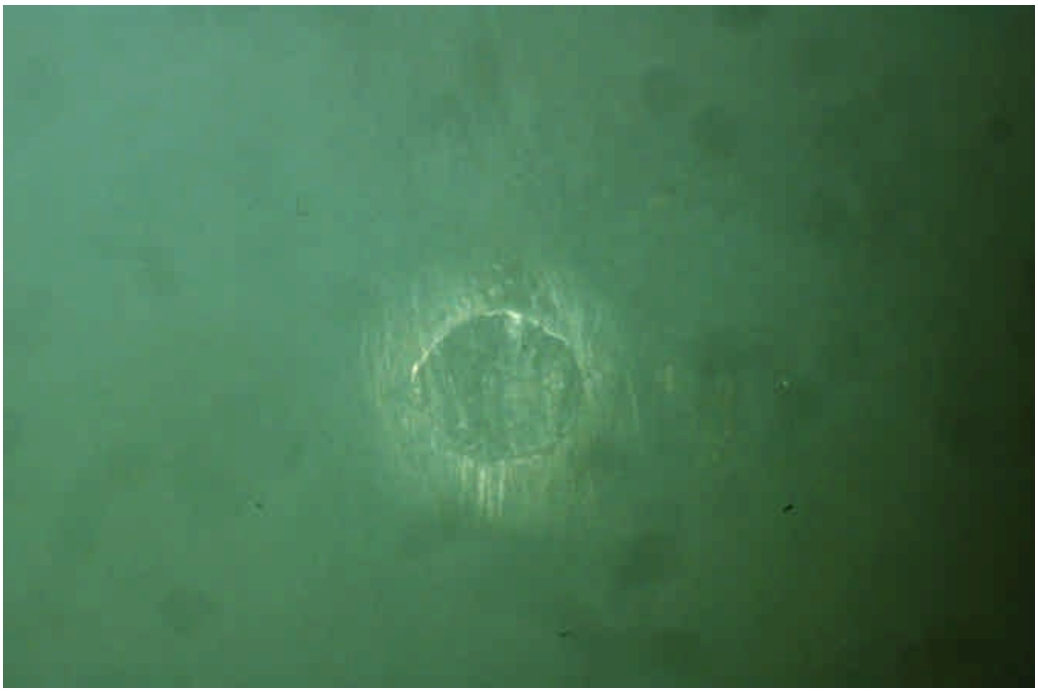

Figure 4.2.3.11 Filtered Dimethyl Terephthalate and Tert-Butyl Hydroquinone in Alumina A System, Test 44: Photomacrograph of Ball Wear Area (40 x)

4.2.4 Caprolactam

Caprolactam represented the cyclic amide class of high temperature anti-wear additives. The average of two tests at 1 wt % resulted in significant wear reductions with the Alumina A System as evidenced by the comparison in Figure 4.2.4.1. Filtration of the particulate matter did not reduce the anti-wear behavior significantly. Photomacrographs of caprolactam wear tests are given in Figures 4.2.4.2 - 9. The wear areas of Figures 4.2.4.2 and 4.2.4.3 reveal a wear track with negligible amounts of debris. Dark bands present on each side mask the directional finishing marks visible inside and far outside the worn area. The fact that finishing marks are still visible within the wear track is additional testimony to the excellent anti-wear behavior of this compound. The crystals seen in both figures grew soon after removing the specimen from the holder.

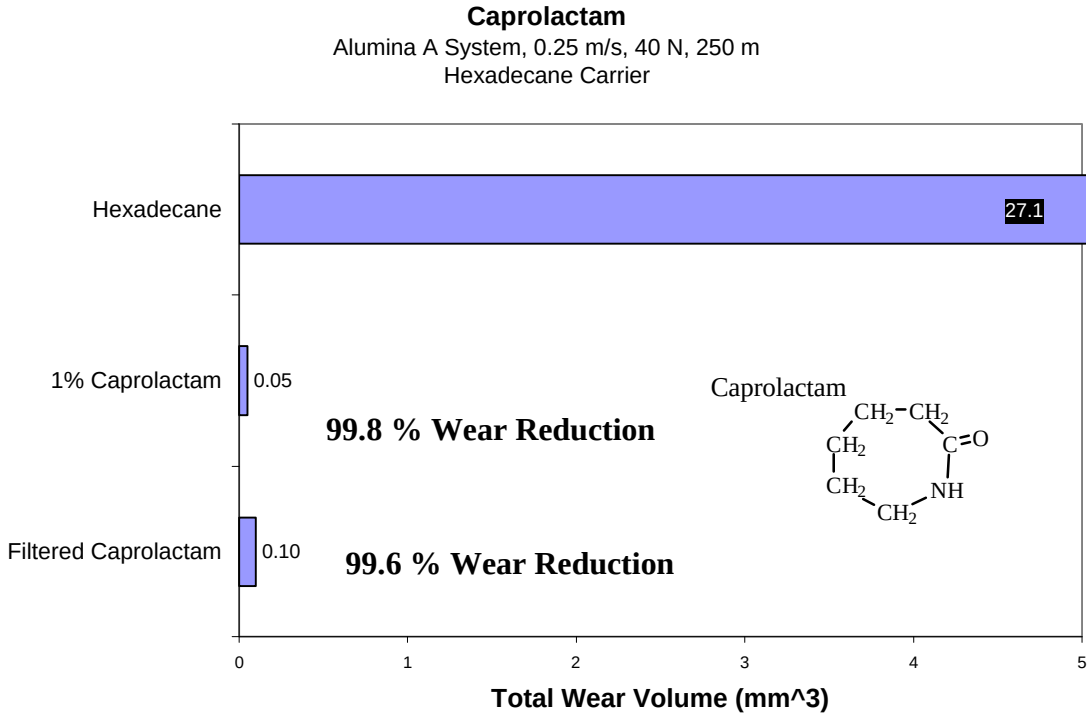

Figure 4.2.4.1 Anti-wear Effects of Caprolactam in Alumina A System

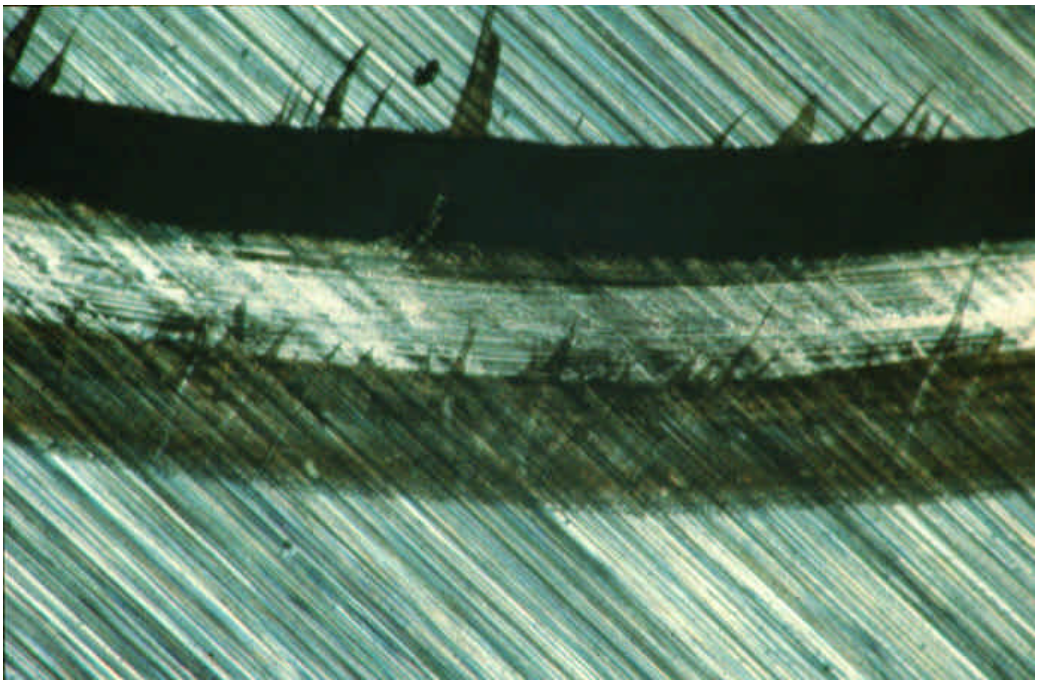

Figure 4.2.4.2 Caprolactam in Alumina A System, Test 30: Photomacrograph of Disk Wear Track (40 x)

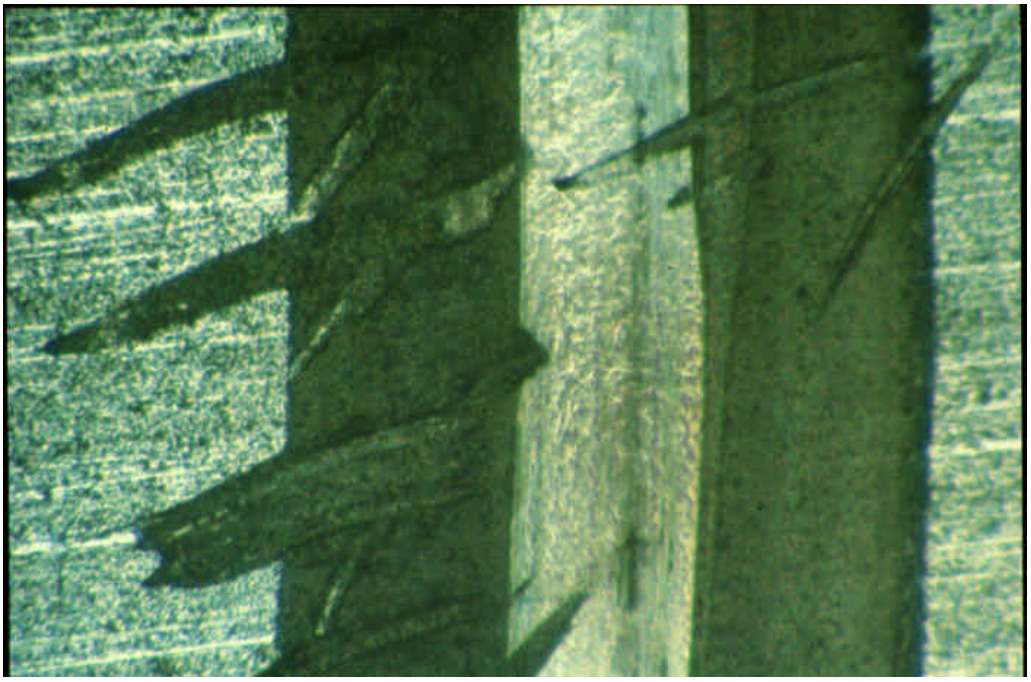

Figure 4.2.4.3 Caprolactam in Alumina A System, Test 31: Photomacrograph of Disk Wear Track (40 x)**.**

Following rinsing, internal lighting on the ball wear area reveals dark nonreflective debris indicative of a residual anti-wear film as seen in Figures 4.2.4.4-5. The ball and disk wear areas of Test 43 shown in Figure 4.2.4.6 demonstrate the effects of using different lighting schemes to reveal the nature of test specimen surfaces. Lighting went from all external (oblique) in the photomacrographs at left to all internal (direct incident) on the right while the center photomacrographs were taken with combined lighting. The same substance around the wear track appears white in the left images and dark in the right images. The right images show how thoroughly the substance covers the surface by providing a good contrast with the reflective areas of the specimens.

Figures 4.2.4.7- 9 present these visual effects for the filtered mixture of caprolactam and hexadecane. The attachment of debris seen in Figures 4.2.4.7 and 4.2.4.8 results in a white powdery film over the disk and ball wear areas respectively. Internal lighting in Figure 4.2.4.9 reveals scattered patches of dark across the reflective worn alumina while interference fringes just outside the ball wear area suggest a clear film like covering.

The high wear Alumina A system results presented above demonstrated the potential of new additives in each of the three classes on ceramic substrates. Next, Section 4.3 presents results of continued ceramic testing across the three new classes of anti-wear additives and several separate parametric studies from the distinctly lower wear Alumina B system.

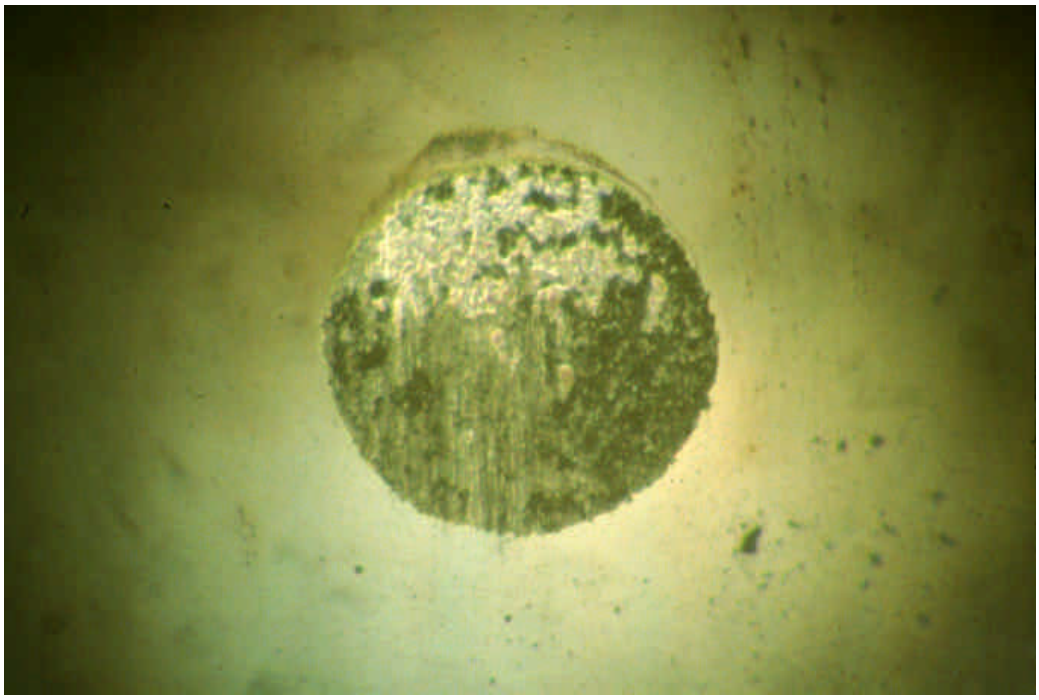

Figure 4.2.4.4 Caprolactam in Alumina A System, Test 30: Photomacrograph of Ball Wear Area (80 x)

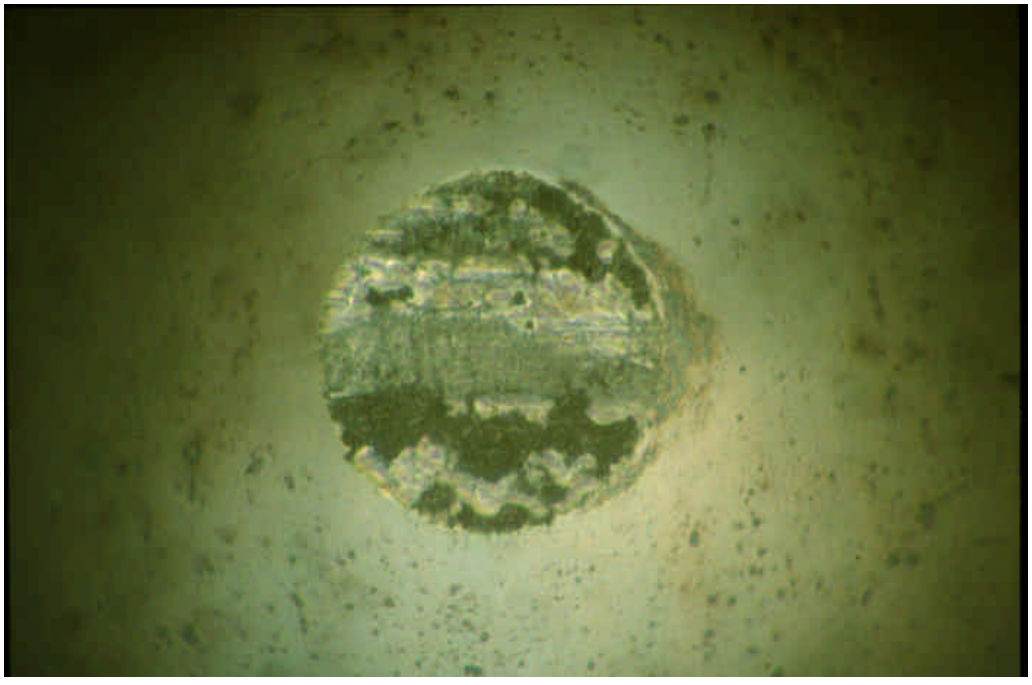

Figure 4.2.4.5 Caprolactam in Alumina A System, Test 31: Photomacrograph of Ball Wear Area (80 x)

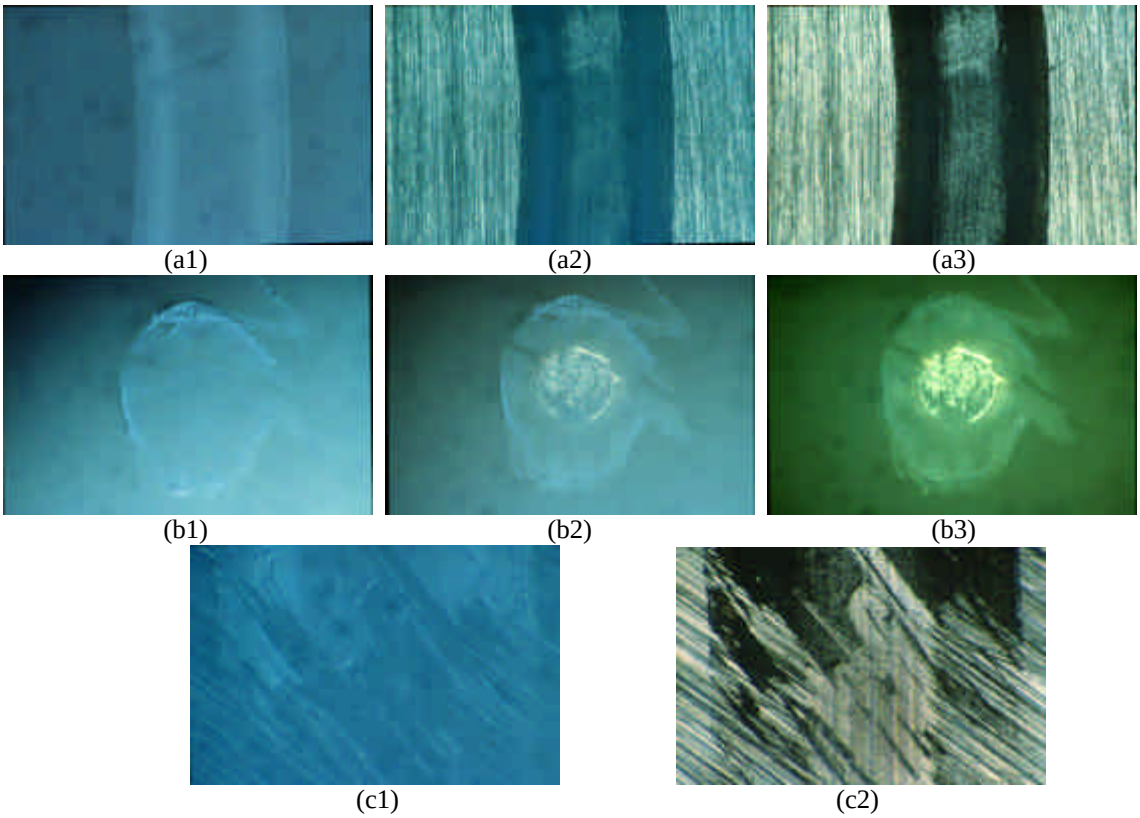

Figure 4.2.4.6 Filtered Caprolactam in Alumina A System, Test 43: Photomacrographs of Wear Areas.

Figure 4.2.4.7 Filtered Caprolactam in Alumina A System, Test 43: Photomacrograph of Ball Wear Area (40 x).

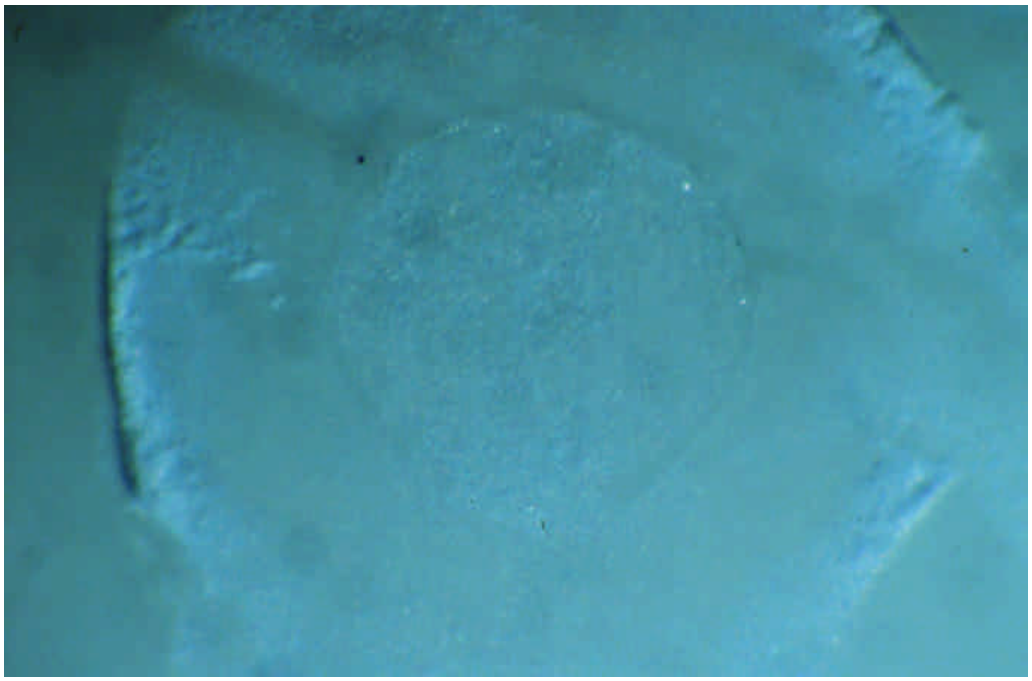

Figure 4.2.4.8 Filtered Caprolactam in Alumina A System, Test 43: Photomacrograph of Ball Wear Area, External Lighting (80 x)

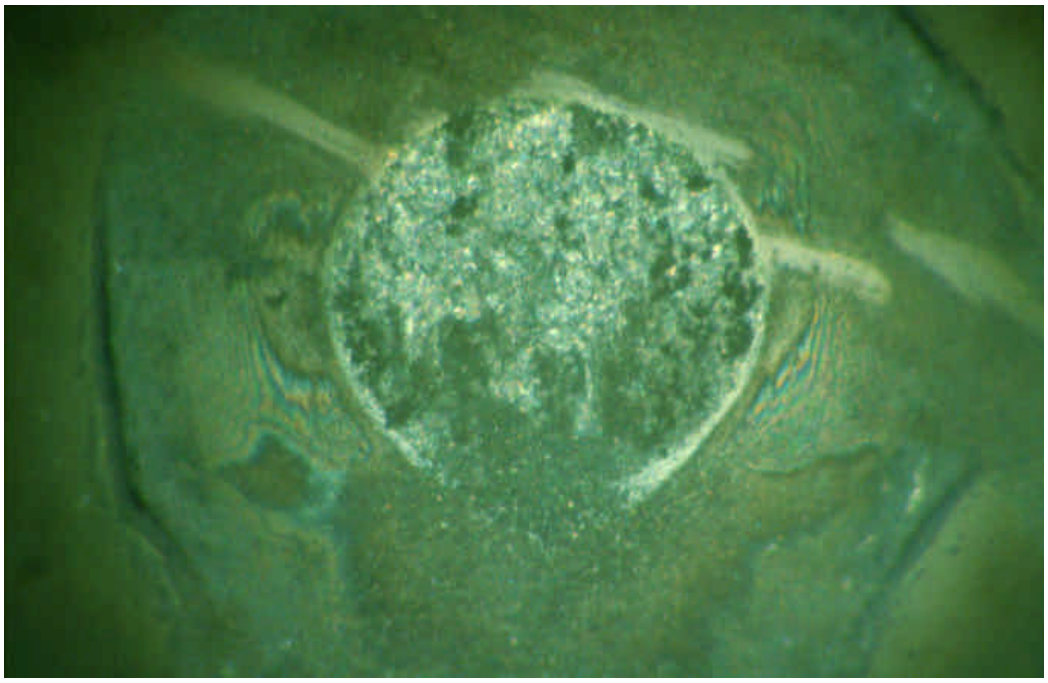

Figure 4.2.4.9 Filtered Caprolactam in Alumina A System, Test 43: Photomacrograph of Ball Wear Area, Internal Lighting (80 x)